



# New Architectures for Designed Catalysts: Selective Oxidation using AgAu Nanoparticles on Colloid-Templated Silica

## Citation

Shirman, Tanya, Judith Lattimer, Mathilde Luneau, Elijah Shirman, Christian Reece, Michael Aizenberg, Robert J. Madix, Joanna Aizenberg, and Cynthia M. Friend. 2017. "New Architectures for Designed Catalysts: Selective Oxidation Using AgAu Nanoparticles on Colloid-Templated Silica." *Chemistry - A European Journal* 24 (8) (November 14): 1833–1837. doi:10.1002/chem.201704552.

## Published Version

doi:10.1002/chem.201704552

## Permanent link

<http://nrs.harvard.edu/urn-3:HUL.InstRepos:37235481>

## Terms of Use

This article was downloaded from Harvard University's DASH repository, and is made available under the terms and conditions applicable to Open Access Policy Articles, as set forth at <http://nrs.harvard.edu/urn-3:HUL.InstRepos:dash.current.terms-of-use#OAP>

## Share Your Story

The Harvard community has made this article openly available.  
Please share how this access benefits you. [Submit a story](#).

[Accessibility](#)

# New architectures for designed catalysts: Selective oxidation using AgAu nanoparticles on colloid-templated silica

Tanya Shirman,<sup>§1,2</sup> Judith Lattimer,<sup>§3</sup> Mathilde Luneau,<sup>3</sup> Elijah Shirman,<sup>1,2</sup> Christian Reece,<sup>3</sup> Michael Aizenberg,<sup>2</sup> Robert J. Madix,<sup>1</sup> Joanna Aizenberg,<sup>\*1,2,3</sup> and Cynthia M. Friend<sup>\*1,3</sup>

<sup>1</sup> John A. Paulson School of Engineering and Applied Sciences, Harvard University, Cambridge, MA 02138, USA. <sup>2</sup>Wyss Institute for Biologically Inspired Engineering, Harvard University, Cambridge, MA 02138, USA. <sup>3</sup>Department of Chemistry and Chemical Biology, Harvard University, Cambridge, MA 02138, USA.

\*Correspondence and requests for materials should be addressed to J.A. (email: [jaiz@seas.harvard.edu](mailto:jaiz@seas.harvard.edu)) and C.M.F. ([friend@fas.harvard.edu](mailto:friend@fas.harvard.edu)).

§These two authors contributed equally to this paper.

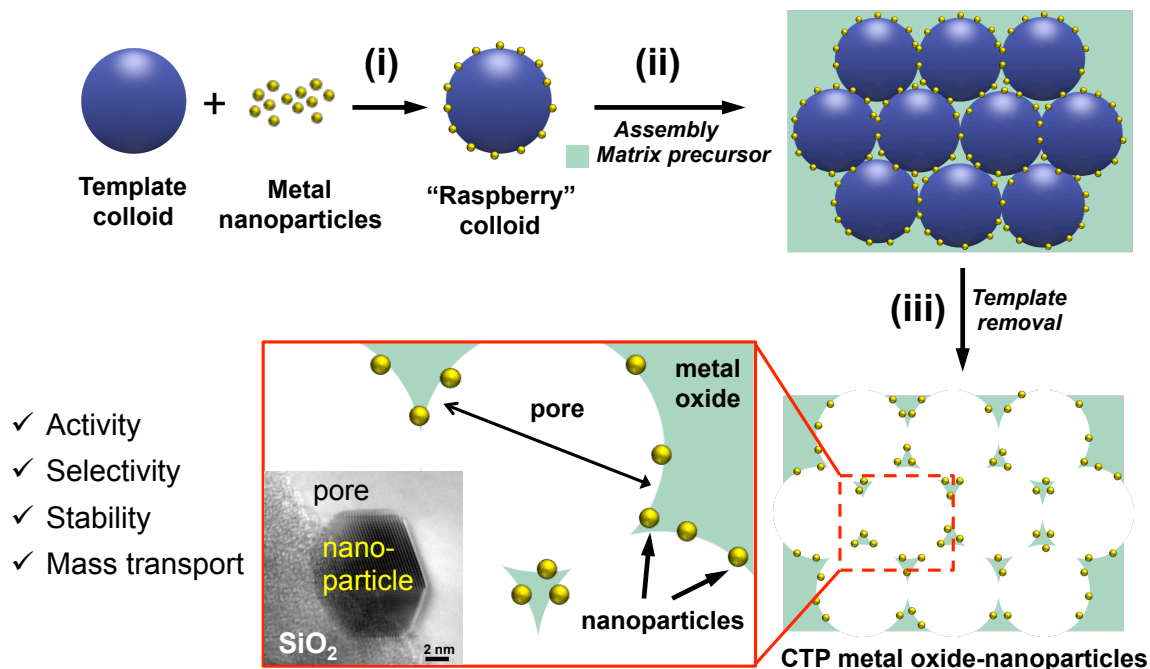
**Abstract:** A highly modular synthesis of designed catalysts with controlled bimetallic nanoparticle size and composition and a well-defined structural hierarchy is demonstrated. Exemplary catalysts—bimetallic dilute Ag-in-Au nanoparticles partially embedded in a porous SiO<sub>2</sub> matrix (SiO<sub>2</sub>-Ag<sub>x</sub>Au<sub>y</sub>)—were synthesized by the decoration of polymeric colloids with the bimetallic nanoparticles followed by assembly into a colloidal crystal backfilled with the matrix precursor and subsequent removal of the polymeric template. We show that these new catalysts architectures are significantly better than nanoporous dilute AgAu alloy catalysts (nanoporous Ag<sub>0.03</sub>Au<sub>0.97</sub>) while retaining a clear predictive relationship between their surface reactivity with that of single crystal Au surfaces. This paves the way for broadening the range of new catalyst architectures required for translating the designed principles developed under controlled conditions to designed catalysts under operating conditions for highly selective coupling of alcohols to form esters. Excellent catalytic performance of the porous SiO<sub>2</sub>-Ag<sub>x</sub>Au<sub>y</sub> structure for selective oxidation of both methanol and ethanol to produce esters with high conversion efficiency, selectivity, and stability was demonstrated, illustrating the ability to translate design principles developed for support-free materials to the colloid-templated structures. The synthetic methodology reported is customizable for the design of a wide range of robust catalytic systems inspired by design principles derived from model studies. Fine control over the composition, morphology, size, distribution and availability of the supported nanoparticles was demonstrated.

Heterogeneous catalysis is of paramount importance for contemporary chemical and energy industries. Hence, the goal of “catalysis by design” has emerged as an important research field that derives inspiration from model studies.<sup>[1]</sup> There are reasons for high interest in designing bimetallic catalytic materials with specific compositions and structural motifs. First, bimetallic nanoparticles often have chemical properties that are distinct from either individual metal; thus, presenting tremendous potential for creating

new, efficient catalysts.<sup>[2]</sup> Second, they are known to provide a clear predictive relationship between their surface reactivity with that of single crystal Au surfaces enabling the ability to translate design principles from controlled conditions to operating conditions.<sup>[3]</sup>

Herein, we demonstrate a modular and versatile approach for the design of an efficient bimetallic catalyst system based on the synthesis of a porous framework of silica with embedded bimetallic AgAu nanoparticles of uniform size and composition. This specific system establishes that catalytic activity and selectivity observed in support-free nanoporous Ag<sub>3</sub>Au<sub>97</sub> alloys<sup>[1a, 3-4]</sup> translates to the embedded nanoparticles; thus, demonstrating that the modular synthesis process can be used to more generally test design principles. Indeed, the AgAu nanoparticles embedded in a colloid-templated porous (CTP) SiO<sub>2</sub> is an active, selective, and robust catalyst for oxidative coupling of alcohols, similar to nanoporous Ag<sub>3</sub>Au<sub>97</sub>. The synthetic procedure is a generalizable platform for the fabrication of a tailored catalysts that enables an optimal design of its composition and morphology.

The fabrication employs modification of colloids with metal nanoparticles, assembly of these “raspberry” colloids into a colloidal crystal monolith and backfilling of the interstitials with a metal oxide matrix precursor material, followed by heat treatment to remove the polymeric template (Scheme 1). This method enables the fabrication of highly porous structures with contiguous, interconnected pores, uniformly decorated with metal nanoparticles. Due to their high modularity, CTP materials can be designed with any size and composition of nanoparticles and customized to have specific pore sizes defined by the size of the sacrificial colloids.<sup>[5]</sup> This approach leads to improved accessibility and stability of the nanoparticles, which are partially grafted into the matrix surface, preventing their sintering and surface diffusion.



**Scheme 1.** Schematic of the synthesis of metal nanoparticles embedded in colloid-templated porous materials, with emphasis on the fully accessible metal nanoparticles placed at the pore/matrix interface and summarizing the advantageous properties provided by this type of material for the design of an efficient heterogeneous catalyst. Inset in the bottom shows a TEM image of a nanoparticle partially entrenched into the silica matrix.

The AgAu bimetallic nanoparticles were synthesized via galvanic replacement using a modification of published procedures.<sup>[6]</sup> The average size of the Ag<sub>x</sub>Au<sub>y</sub> nanoparticles increased with the increasing Au content, as reported previously (Figure 1A,B, S1; Table S1).<sup>[6b, 7]</sup> The composition of the nanoparticles was determined using inductively coupled plasma mass spectrometry (ICP-MS). Silver is concentrated on or near the surface of the nanoparticles based on Scanning Transmission Electron Microscopy-Energy Dispersive X-ray Spectroscopy (STEM-EDS) measurements (Figure 1C, S2); the centers of individual AgAu nanoparticles are enriched in Au, based on the cross-section scan (Figure S3).

The AgAu nanoparticles were attached to the surface of polystyrene colloids (385 nm) to form composite “raspberry” colloids, which were used as sacrificial templates in the synthesis of CTP silica catalyst (Scheme 1, Figures 1D and S4). The material resulting from the CTP synthesis has AgAu nanoparticles incorporated into a macroporous silica matrix with 375±5 nm voids interconnected by ~80 nm windows. The AgAu nanoparticles were homogeneously distributed at the interface (Figure 1E, S5, S6). The remarkable robustness and high-temperature stability of the material are demonstrated by the fact that the size and distribution of the metal nanoparticles was preserved after calcination at 500 °C in air (Figure 1F, S6, Table S1). In contrast, nanoparticles covalently immobilized on the surface of preformed CTP SiO<sub>2</sub> structures rapidly sinter upon

calcination of the structure leading to an increase in the nanoparticle diameter from  $4.2\pm 0.4$  to  $19.3\pm 5.8$  nm (Figure S7). Together, these results demonstrate that partial embedding of the nanoparticles in the silica impart a high degree of thermal stability to the catalyst structure.

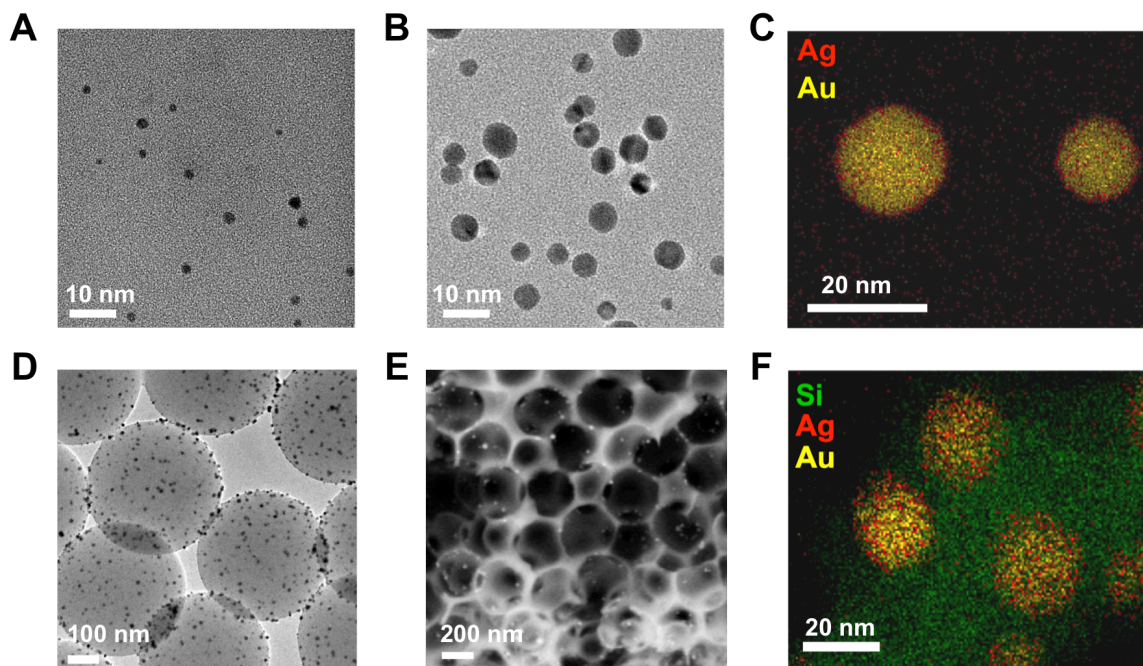


**Figure 1** TEM images of: (A)  $\text{Ag}_{50}\text{Au}_{50}$  nanoparticles and (B)  $\text{Ag}_{10}\text{Au}_{90}$  nanoparticles. (C) STEM-EDS map of  $\text{Ag}_{10}\text{Au}_{90}$  nanoparticles. (D) TEM image of raspberry colloids  $\text{PS}@Ag_{10}Au_{90}$ . (E) SEM image of CTP  $\text{SiO}_2\text{-Ag}_{10}\text{Au}_{90}$  (white dots are metal nanoparticles). (F) STEM-EDS map of CTP  $\text{SiO}_2\text{-Ag}_{10}\text{Au}_{90}$ , showing uniform size and metal distribution after calcination at  $500^\circ\text{C}$  in air.

The CTP  $\text{SiO}_2\text{-Ag}_x\text{Au}_y$  catalysts required activation by ozone followed by flowing reactants prior to driving the oxidative coupling of methanol in a process similar to that for free-standing nanoporous  $\text{Ag}_3\text{Au}_{97}$  (npAu).<sup>[1a]</sup> As-prepared catalysts had very low activity (Figure 2A); however, once activated, the catalysts selectively transformed methanol to form methyl formate (Figure 2B, Table 1). Typically, the methyl formate yield increased smoothly over  $\sim 7$  h following ozone treatment, and was stable thereafter for over 40 h, the end of the testing period (Figure 2B). For example, CTP  $\text{SiO}_2\text{-Ag}_{10}\text{Au}_{90}$  stabilized at 35% conversion of methanol with a selectivity of 90% for methyl formate (Figure 2B). The only other product detected was  $\text{CO}_2$ . Conversion and selectivity calculations can be found in the SI. Understanding the catalyst activation will require further study. Similar activation of npAu leads to enrichment of the surface in Ag to form an alloy that triggers the dissociation of  $\text{O}_2$ .<sup>[8]</sup> Further study is required to fully understand the underlying reasons for the induction period.

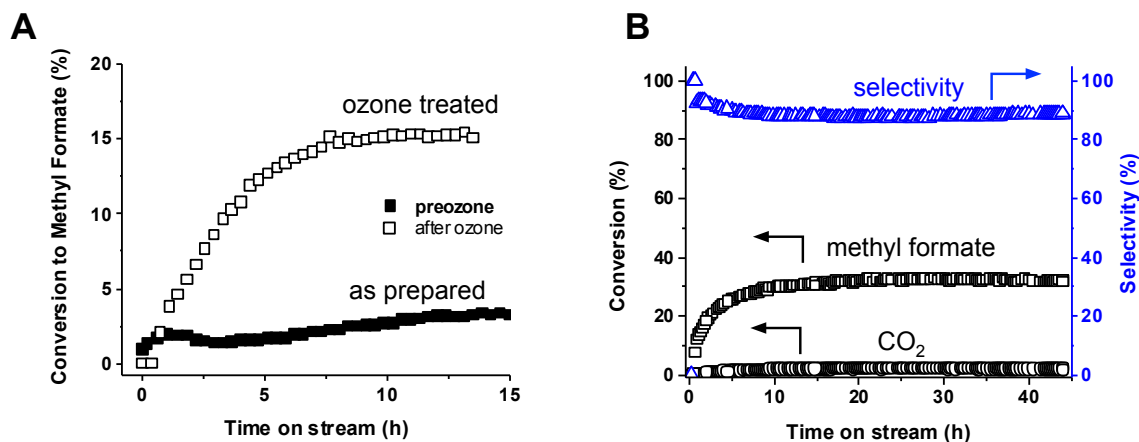


**Figure 2** (A) Conversion of methanol to methyl formate using CTP SiO<sub>2</sub>-Ag<sub>10</sub>Au<sub>90</sub> (nanoparticle wt. 4.4 mg) as prepared (closed squares) and after ozone treatment (open squares). (B) Conversion of methanol to methyl formate (MF, black squares) and carbon dioxide (CO<sub>2</sub>, black circles) and selectivity for methyl formate (blue triangles) using CTP SiO<sub>2</sub>-Ag<sub>10</sub>Au<sub>90</sub> (nanoparticle wt. 3.3 mg) immediately following ozone treatment. Reaction conditions: 6 mol% methanol and 20 mol% O<sub>2</sub> in He at flow rate 50 ml/min at 423 K.

There was no conversion of methanol detected for the CTP SiO<sub>2</sub> matrix without metal nanoparticles (Figure S8). The most active catalyst composition among those screened exhibited nearly five times the activity per unit weight of metal compared to the best-performing npAu under the same conditions, albeit with slightly lower selectivity (Table 1, Figure S9). The lower selectivity may be due to the higher Ag content in the CTP SiO<sub>2</sub>-Ag<sub>x</sub>Au<sub>y</sub> catalysts (10 mol% in the AgAu nanoparticles vs 1-3 mol% in npAu).<sup>[1a]</sup> Previous work on npAu with 10 mol% Ag showed only complete combustion to CO<sub>2</sub> (Table S2).<sup>[4]</sup>

The generality of the oxidation catalysis driven by CTP-Ag<sub>10</sub>Au<sub>90</sub> was demonstrated by the activity for oxidative coupling of methanol and ethanol (Figure 3, Table 1). Only esters and acetaldehyde were produced; no CO<sub>2</sub> was detected. The product distributions measured as a function of methanol mole fraction showed that excess methanol (~80%) is required for maximum production of methyl acetate, similar to npAg<sub>0.03</sub>Au<sub>0.97</sub> under similar conditions.<sup>[9]</sup> The dependence of the selectivity for acetaldehyde production decreased both as the total alcohol concentration increased from 2 to 10% and as the temperature was increased up to 240 °C (Figure S10), also analogous to npAg<sub>0.03</sub>Au<sub>0.97</sub>.<sup>[9]</sup> There are, though, differences between the catalysts: The CTP-Ag<sub>10</sub>Au<sub>90</sub> produced significantly more acetaldehyde<sup>[9]</sup> and the rate of ethanol conversion was 3-4 times higher for the CTP SiO<sub>2</sub>-Ag<sub>10</sub>Au<sub>90</sub> catalyst (0.018 mmol g<sup>-1</sup> s<sup>-1</sup>) than for npAu under the same conditions (0.004 mmol g<sup>-1</sup> s<sup>-1</sup>, Table S2). Further study is required to understand these differences in detail, although the compositional difference most likely plays a role.

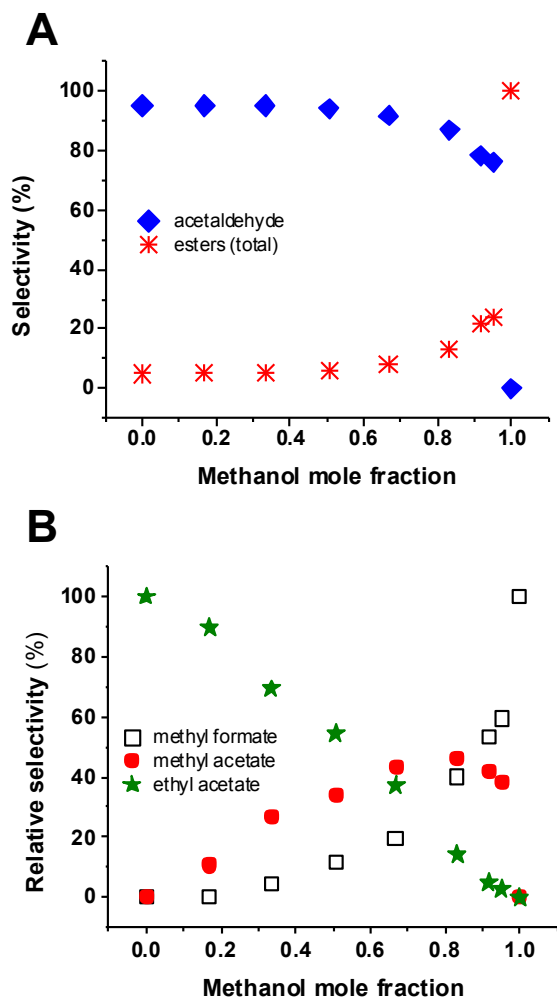


**Figure 3.** The general ability for the CTP-SiO<sub>2</sub>-Ag<sub>10</sub>Au<sub>90</sub> to catalyze alcohol oxidation is demonstrated by the activity for selective oxidation of mixtures of methanol and ethanol. The dependence of selectivity on the methanol mole fraction for oxidation of various mixtures of methanol and ethanol over CTP-SiO<sub>2</sub>-Ag<sub>10</sub>Au<sub>90</sub> (nanoparticle wt. 5.7 mg) using O<sub>2</sub> as an oxidant shows that a high methanol mole fraction is required to maximize the formation of the methyl ester. This behavior is qualitatively similar to the performance of nanoporous Ag<sub>3</sub>Au<sub>97</sub>. (A) The selectivity for formation of the products: acetaldehyde and esters (the sum of methyl formate, methyl acetate, and ethyl acetate). (B) Relative selectivity for production of the various esters (methyl formate, ethyl acetate, and methyl acetate). Reaction conditions: 6% total alcohol, 20% oxygen in He, 50 ml/min flow, 423 K. No CO<sub>2</sub> is detected in any of these experiments.

The long-term stability of CTP SiO<sub>2</sub>-Ag<sub>10</sub>Au<sub>90</sub> was demonstrated by assessing its activity by repeated measurements over a period of 6 months (Figure 4A). Although the sample was occasionally removed from the reactor and exposed to ambient conditions, no additional ozone activation was required: the sample was only activated *once*—at the beginning of the first experiment. After reintroduction into the reactor, selectivity

decreased somewhat, but was largely recovered under reaction conditions after 24 h. Consistent with this stable catalytic performance, there were no significant morphological or compositional changes detected by SEM, TEM and ICP-MS after catalysis (Figure S11, Table S1). The catalytic performance at higher temperatures (up to 240 °C) showed increased methanol conversion accompanied by a drastic decrease in selectivity for methyl formate (Figure S12). The fact that the catalyst performance does not change over long periods of time, without special efforts to store it in a controlled atmosphere and without the need to reactivate between uses, is in and of itself a very valuable result.

**Table 1** Reaction rates and selectivities of npAu and CTP SiO<sub>2</sub>-AgAu catalysts.<sup>a</sup>

Catalyst composition <sup>b</sup>		Rate of methanol conversion, <sup>c</sup> mmol s <sup>-1</sup> g <sup>-1</sup>	Selectivity to methyl formate, <sup>c</sup> %
npAu	foils	0.055	95
	Ag <sub>10</sub> Au <sub>90</sub>	0.23	90
CTP SiO <sub>2</sub>	Ag <sub>20</sub> Au <sub>80</sub>	0.07	100
	Ag <sub>50</sub> Au <sub>50</sub>	0.02	100

<sup>a</sup>Catalysts were treated with flowing ozone and then kept in reaction conditions for at least 24 h to ensure stability, and those are the rates and selectivities reported here. Rates are calculated on a per gram of metal basis.

<sup>b</sup>Composition of CTP-SiO<sub>2</sub> catalysts determined from ICP-MS measured after reaction. Details in SI.

<sup>c</sup>Conditions: 6 mol% methanol and 20 mol% O<sub>2</sub> in He; flow rate 50 ml/min; 423 K.

The catalyst architecture is free from diffusional limitations in rate under reaction conditions based on several analyses. First, controlled variation of catalyst loading (9, 30, and 36 mg of CTP SiO<sub>2</sub>-Ag<sub>10</sub>Au<sub>90</sub> with 15 wt% nanoparticles) shows catalytic performance consistent with reaction-limited behavior (Figure 4B, squares). Second, independently measured activities of three CTP SiO<sub>2</sub>-Ag<sub>10</sub>Au<sub>90</sub> catalysts with varied nanoparticle content (10, 16, and 21 wt%) were found to increase linearly with increasing nanoparticle loading (Figure 4B, diamonds). Third, the estimated Weisz modulus and Carberry number (Tables S2, S4, S5) were at least one order of magnitude lower than the threshold values characteristic of diffusional limitations.<sup>[10]</sup> Fourth, the activity of the catalyst remained constant as the flow rate and volume of catalyst were varied in concert, maintaining constant space velocity, between 80 ml/min and 50 ml/min. Only below a flow rate of 50 ml/min was there a decrease in conversion, indicating that there was no external diffusion limitation under reaction conditions.<sup>[11]</sup> Finally, the activity of the catalyst did not increase as the catalyst macro-particle size was decreased systematically, indicating that the reaction rate was not pore-diffusion-limited under these conditions (Table S3, Figure S13).<sup>[11]</sup>



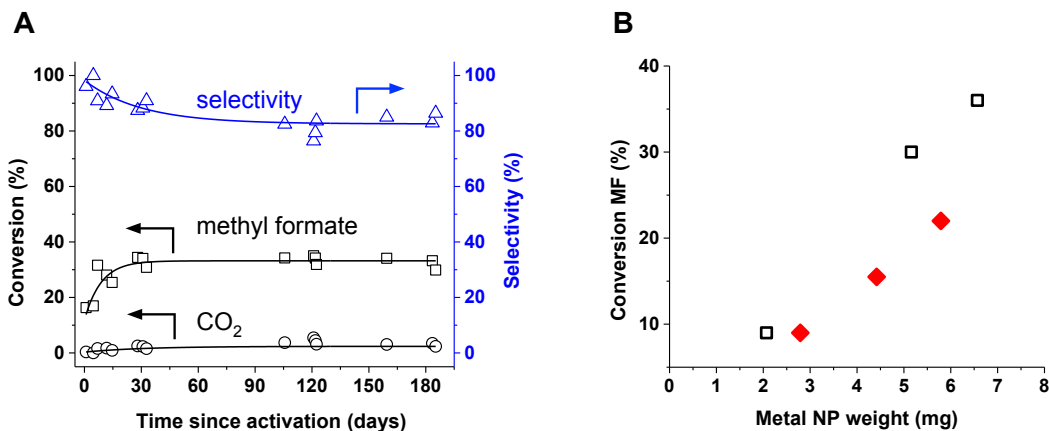


**Figure 4** (A) Steady-state conversion of methanol to methyl formate (MF, black squares) and carbon dioxide (CO<sub>2</sub>, black circles) and selectivity to methyl formate (blue triangles) using CTP SiO<sub>2</sub>-Ag<sub>10</sub>Au<sub>90</sub> (nanoparticle wt. 5.2 mg). (B) Methanol conversion to methyl formate as a function of total metal nanoparticle loading in the reactor. The squares correspond to 9, 30, and 36 mg of CTP SiO<sub>2</sub>-Ag<sub>10</sub>Au<sub>90</sub> prepared with with 15 wt% nanoparticles (□). The diamonds correspond to 28 mg of CTP SiO<sub>2</sub>-Ag<sub>10</sub>Au<sub>90</sub> prepared with 10, 16, and 21 wt% nanoparticles (◆). Reaction conditions: 6 mol% methanol, 20 mol% O<sub>2</sub> in He; flow rate 50 mL/min; 423 K.

In conclusion, AgAu nanoparticles incorporated into colloid-templated porous materials are robust catalysts for selective alcohol oxidative coupling, similar to npAu. The advantage of the colloid template method used here is that it is a highly versatile and tunable approach for synthesizing a library of bimetallic catalyst materials without mass transport limitations. This first demonstration of the catalytic activity of CTP SiO<sub>2</sub>-Ag<sub>x</sub>Au<sub>y</sub> for selective oxidative coupling of methanol to form methyl formate provides clear evidence that controlled incorporation of the bimetallic nanoparticles yields an extremely robust catalyst—both in catalyst performance and in structural integrity.

Despite many similarities, there are key differences in the catalytic behavior of the CTP SiO<sub>2</sub>-Ag<sub>x</sub>Au<sub>y</sub> and npAu. Notably, in npAu increasing the overall Ag content to 10% leads to complete combustion with low conversion rates (Table S2).<sup>[4]</sup> In contrast, a higher Ag content in the nanoparticle catalyst decreases its per gram activity, but the selectivity remains high. These differences may be due to effects of the support, e.g. incorporation of Ag into a silicate<sup>[12]</sup> and/or due to differences in the distribution of the Ag in the near-surface region.<sup>17</sup> Future investigations are in progress to probe the role of Ag in the CTP SiO<sub>2</sub>-Ag<sub>x</sub>Au<sub>y</sub> catalysts. It is noteworthy that while both catalytic systems show excellent activity at mild conditions, the important feature of CTP SiO<sub>2</sub>-Ag<sub>10</sub>Au<sub>90</sub> in comparison to npAu is the substantial increase in conversion coupled with significant reduction in metal content. In addition, the considerably higher stability of the CTP catalysts towards high temperatures allows for a wider range of reaction conditions, potentially allowing one to access reaction products or increase selectivities beyond the capability of npAu.

The impact of this work lies in the modularity of the synthesis described here as a platform for making and testing a plethora of *rationally designed catalysts* with controlled bimetallic nanoparticle size and composition and a well-defined structural and compositional hierarchy. The synthesis provides the ability to systematically vary the nature of the metal oxide support, the pore size and structure, and the composition, size, loading and placement of the single or multi-metallic nanoparticles (Figure S14).<sup>[13]</sup> Hence, novel catalyst materials can be produced for a broad range of catalyst compositions and for a wide variety of reactions. The robustness of these catalysts that show no sintering or agglomeration of the nanoparticles is an added benefit. This approach to the design of bimetallic nanoparticle catalysts opens immense possibilities in terms of tailoring the catalyst composition towards efficient and selective chemical transformations in a sustainable and material-efficient way.

### Acknowledgements

This work was supported as part of the Integrated Mesoscale Architectures for Sustainable Catalysis, an Energy Frontier Research Center funded by the U.S. Department of Energy, Office of Science, Basic Energy Sciences under award #DE-SC0012573. T.S. acknowledges support from the Weizmann Institute of Science – National Postdoctoral Award Program for Advancing Women in Science. Electron microscopy were performed at the Center for Nanoscale Systems (CNS) at Harvard University, supported by the NSF under award number ECS-0335765.

Keywords: nanoparticles, colloid templated porous materials, heterogeneous catalysis, selective oxidation, gold, silver.

### References:

- [1] a) M. L. Personick, B. Zugic, M. M. Biener, J. Biener, R. J. Madix and C. M. Friend, *ACS Catalysis* **2015**, *5*, 4237-4241; b) L.-C. Wang, M. L. Personick, S. Karakalos, R. Fushimi, C. M. Friend and R. J. Madix, *Journal of Catalysis* **2016**, *344*, 778-783; c) B. Zugic, S. Karakalos, K. J. Stowers, M. M. Biener, J. Biener, R. J. Madix and C. M. Friend, *ACS Catalysis* **2016**, *6*, 1833-1839.
- [2] a) S. Hermans, T. Khimyak, R. Raja, G. Sankar, J. M. Thomas and B. F. G. Johnson in *Molecular mixed-metal clusters as precursors for highly active supported bimetallic nanoparticles*, Vol. 1 Eds.: B. Zhou, S. Hermans and G. A. Somorjai), **2004**, pp. 33-49; b) R. Ferrando, J. Jellinek and R. L. Johnston, *Chemical Reviews* **2008**, *108*, 845-910; c) M. Sankar, N. Dimitratos, P. J. Miedziak, P. P. Wells, C. J. Kiely and G. J. Hutchings, *Chemical Society Reviews* **2012**, *41*, 8099-8139; d) A. K. Singh and Q. Xu, *ChemCatChem* **2013**, *5*, 652-676; e) I. Notar Francesco, F. Fontaine-Vive and S.

- Antoniotti, *ChemCatChem* **2014**, *6*, 2784-2791; f) A. S. Duke, K. Xie, J. R. Monnier and D. A. Chen, *Surface Science* **2017**, *657*, 35-43.
- [3] M. L. Personick, M. M. Montemore, E. Kaxiras, R. J. Madix, J. Biener and C. M. Friend, *Philos Trans A Math Phys Eng Sci* **2016**, *374*.
- [4] A. Wittstock, V. Zielasek, J. Biener, C. M. Friend and M. Bäumer, *Science* **2010**, *327*, 319-322.
- [5] K. R. Phillips, G. T. England, S. Sunny, E. Shirman, T. Shirman, N. Vogel and J. Aizenberg, *Chem Soc Rev* **2016**, *45*, 281-322.
- [6] a) W. Shi, Y. Sahoo, M. T. Swihart and P. N. Prasad, *Langmuir* **2005**, *21*, 1610-1617; b) J. D. Padmos, M. Langman, K. MacDonald, P. Comeau, Z. Yang, M. Filiaggi and P. Zhang, *The Journal of Physical Chemistry C* **2015**, *119*, 7472-7482.
- [7] S. Ristig, O. Prymak, K. Loza, M. Gocyla, W. Meyer-Zaika, M. Heggen, D. Raabe and M. Epple, *Journal of Materials Chemistry B* **2015**, *3*, 4654-4662.
- [8] B. Zugic, L. Wang, C. Heine, D. N. Zakharov, B. A. J. Lechner, E. A. Stach, J. Biener, M. Salmeron, R. J. Madix and C. M. Friend, *Nat Mater* **2017**, *16*, 558-564.
- [9] L.-C. Wang, K. J. Stowers, B. Zugic, M. L. Personick, M. M. Biener, J. Biener, C. M. Friend and R. J. Madix, *Journal of Catalysis* **2015**, *329*, 78-86.
- [10] a) G. F. Froment and K. B. Bischoff, *Chemical Reactor Analysis and Design*, J. Wiley & Sons, New York, **1990**, p; b) J. J. Carberry in *Catalysis, Science and Technology*, Vol. 8 Eds.: J. R. Anderson and M. Boudart), Springer, Berlin, **1987**, pp. 131-172.
- [11] C. Perego and S. Peratello, *Catalysis Today* **1999**, *52*, 133-145.
- [12] a) A. M. Shor, S. S. Laletina, E. A. Ivanova Shor, V. A. Nasluzov, V. I. Bukhtiyarov and N. Rösch, *Surface Science* **2014**, *630*, 265-272; b) S. Pramanik, S. Chattopadhyay, J. K. Das, U. Manju and G. De, *Journal of Materials Chemistry C* **2016**, *4*, 3571-3580.
- [13] E. Shirman, T. Shirman, A. V. Shneidman, A. Grinthal, K. R. Phillips, H. Whelan, E. Bulger, M. Abramovitch, J. Patil, R. Nevarez and J. Aizenberg, *Advanced Functional Materials* accepted.